Electronic Supplementary Material (ESI) for New Journal of Chemistry.

Supplementary Information

Di- and tetramethoxy benzothienobenzothiophenes: Substitution position effects on the intermolecular interactions, crystal packing and transistor properties

Toshiki Higashino, Akira Ueda, and Hatsumi Mori**

E-mail: t-higashino@aist.go.jp
hmori@issp.u-tokyo.ac.jp

The Institute for Solid State Physics, The University of Tokyo, Kashiwanoha, Kashiwa, Chiba 277-8581, Japan.

General

Commercially available materials were used as received. Anhydrous tetrahydrofuran was purchased from Wako Pure Chemical Industries. All reactions were conducted under argon atmosphere. For thin-layer chromatography (TLC) analysis, Merck pre-coated glass plates (TLC Silica gel 60 F254) were used. Silica gel for column chromatography (Silica Gel 60 N (spherical, neutral), 63−210 μm) was purchased from Kanto chemical. ^{1}H NMR (300 MHz) and ^{13}C NMR (75 MHz) spectra were measured with a JEOL JNM-AL300 spectrometer with $CDCl_3$ as a solvent using Me_4Si or residual solvent as an internal standard. Melting points were measured with a hot-stage apparatus. Elemental analyses were performed at the Department of Chemistry, Graduate School of Science, the University of Tokyo.

Synthesis

[(2-Bromo-4,5-dimethoxyphenyl)ethynyl]trimetylsilane (2b)

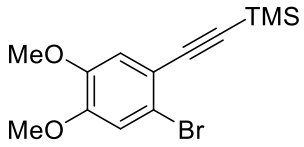

2b

To a mixture of bis(triphenylphosphine)palladium(II) dichloride (1.12 g, 1.60 mmol, 4 mol%), copper(I) iodide (0.609 g, 3.20 mmol, 8 mol%), 1-Bromo-2-iodo-4,5-dimethoxybenzene (**1b**)[14] (13.7 g, 40.0 mmol, 1 eq.), and triethylamine (11.1 mL, 80 mmol, 2 eq.) in dry tetrahydrofuran (50 mL) was added dropwise a solution of trimethylsilylacetylene (8.30 mL, 60.0 mmol, 1.5 eq.) in dry tetrahydrofuran (15 mL) over a period of 10 min at room temperature, and then the resulting mixture was refluxed for 5 h. After cooling down to room temperature, the reaction mixture was filtered through Celite. The filtrate was evaporated under reduced pressure. The residue was subjected to silica gel column chromatography (dichloromethane:hexane = 1:2, R_f = 0.3). The resulting orange solid was washed with methanol, to afford **2b** (11.0 g, 35 mmol, yield 88%) as a white solid. ^{1}H NMR (300 MHz, $CDCl_3$) δ 7.01 (s, 1H), 6.96 (s, 1H), 3.87 (s, 3H), 3.86 (s, 3H), 0.27 (s, 9H).

1-bromo-2-ethynyl-4,5-dimethoxybenzene (3b)

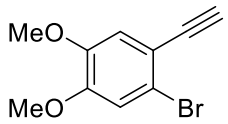

3b

To a methanol-dichloromethane solution (90 mL, 2:1 v/v) of **2b** (9.80 g, 31.3 mmol, 1 eq.) was added potassium carbonate (13.0 g, 93.8 mmol, 3 eq.), and the resulting mixture was stirred at room temperature for 3 h. The reaction mixture was poured into water, and extracted with dichloromethane (50 mL × 3). The combined organic layer was washed with brine, dried over sodium sulfate, filtered, and concentrated under reduced pressure. The residue was subjected to silica gel column chromatography (dichloromethane:hexane = 1:1, R_f = 0.4), to afford **3b** (6.7 g, 28 mmol, yield 89%) as a white solid. ^{1}H NMR (300 MHz, $CDCl_3$) δ 7.03 (s, 1H), 6.99 (s, 1H), 3.89 (s, 3H), 3.86 (s, 3H), 3.29 (s, 1H).

1,2-Bis(2-bromo-4,5-dimethoxyphenyl)ethylene (6)

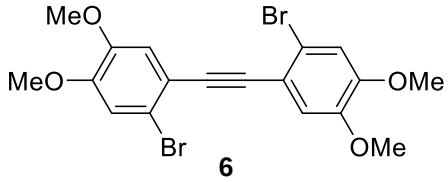

6

To a mixture of bis(triphenylphosphine)palladium(II) dichloride (0.56 g, 0.80 mmol, 4 mol%), copper(I) iodide (0.30 g, 1.6 mmol, 8 mol%), 1-Bromo-2-iodo-4,5-dimethoxybenzene (**1b**)[14] (6.86 g, 20.0 mmol, 1 eq.), and triethylamine (5.5 mL, 40 mmol, 2 eq.) in dry tetrahydrofuran (50 mL) was added dropwise a solution of 1-bromo-2-ethynyl-4,5-dimethoxybenzene (**3b**) (5.30 g, 22.0 mmol, 1.1 eq.) in dry tetrahydrofuran (50 mL) over a period of 5 min at room temperature, and then resulting mixture was refluxed for 15 h. After cooling down to room temperature, the reaction mixture was filtered through Celite. The filtrate was evaporated under reduced pressure, and then the residue was dissolved in dichloromethane, washed with a saturated aqueous solution of ammonium chloride, water, and brine. Then, the organic layer was dried over sodium sulfate, filtered, and concentrated under reduced pressure. The residue was subjected to silica gel column chromatography (dichloromethane:hexane = 1:1, R_f = 0.3; gradually increase the polarity of the mobile phase to dichloromethane). The resulting yellow solid was recrystallized from ethyl acetate to afford **6** (7.8 g, 17 mmol, yield 86%) as a pale yellow solid. M.p. 184−185 °C; ^{1}H NMR (300 MHz, $CDCl_3$) δ 7.07 (s, 2H), 7.06 (s, 2H), 3.90 (s, 12H).

2,3,8,9-Tetramethoxy-benzo[*e*]benzo[4,5]thieno[3,2-*c*][1,2]dithiine (7)

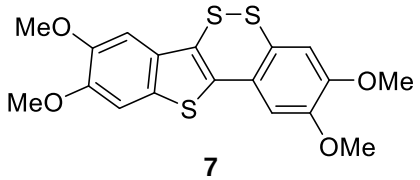

7

To a tetrahydrofuran solution (60 mL) of **6** (2.74 g, 6.00 mmol, 1 eq.) was added dropwise a solution of *t*-butyl lithium in *n*-pentane (1.69 M, 14.2 mL, 24.0 mmol, 4 eq.) at −78 °C. After stirred for at −78 °C 1 h, sulfur powder (0.577 g, 18.0 mmol, 3 eq.) was added. The mixture was gradually warmed up to room temperature over 3 h and then stirred at room temperature for 8 h. The mixture was quenched with a 2 M sodium hydroxide aqueous solution, followed by addition of potassium

hexacyanoferrate(III) (7.90 g, 24.0 mmol, 4 eq.). The resulting mixture was extracted with dichloromethane (50 mL × 3). The combined organic layer was washed with water and brine, dried over sodium sulfate, filtered, and concentrated under reduced pressure. The residue was subjected to silica gel column chromatography (dichloromethane:hexane = 2:1, R_f = 0.3; gradually increase the polarity of the mobile phase to dichloromethane). The resulting fraction was concentrated under reduced pressure, and the residue was washed with methanol, to afford **7** (0.92 g, 2.3 mmol, yield 39%) as an orange powder. M.p. 194−195 °C; ^{1}H NMR (300 MHz, $CDCl_3$) δ 7.26 (s, 1H), 7.13 (s, 1H), 6.99 (s, 1H), 6.97 (s, 1H), 3.99 (s, 3H), 3.98 (s, 3H), 3.96 (s, 3H), 3.93 (s, 3H); Elemental analysis Calcd for $C_{18}H_{16}O_4S_3$: C, 55.08; H, 4.11; N, 0.00. Found: C, 54.99; H, 4.34; N, 0.00.

2,3,7,8-Tetramethoxy-[1]benzothieno[3,2-*b*][1]benzothiophene (BTBT(OMe)$_4$)

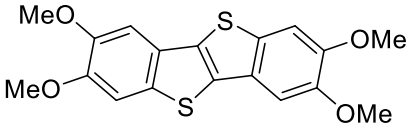

BTBT(OMe)$_4$

The mixture of **7** (0.235 g, 0.600 mmol, 1 eq.) and copper nanopowder (0.153 g, 2.40 mmol, 4 eq.) was stirred at 250 °C for 20 min. After the mixture was cooled down to room temperature, dichloromethane was added to the mixture, and the insoluble materials were removed by filtration through Celite. The filtrate was concentrated under reduced pressure, and the residue was washed with methanol and then recrystallized from ethyl acetate to afford **BTBT(OMe)$_4$** (0.18 g, 0.50 mmol, yield 83%) as colorless crystals. M.p. >300 °C; ^{1}H NMR (300 MHz, $CDCl_3$) δ 7.35 (s, 2H), 7.23 (s, 2H), 4.02 (s, 3H), 3.99 (s, 3H) ppm; ^{13}C NMR (75 MHz, $CDCl_3$) δ 148.4, 148.0, 133.9, 131.8, 126.9, 105.7, 102.8, 56.5, 56.0; Elemental analysis Calcd for $C_{18}H_{16}O_4S_2$: C, 59.98; H, 4.47; N, 0.00. Found: C, 59.90; H, 4.60; N, 0.00.

Redox properties

Cyclic voltammograms were measured on ALS model 610DB electrochemical analyzer in an acetonitrile solution containing 0.1 M tetra-*n*-butylammonium hexafluorophosphate (*n*-$Bu_4 \cdot PF_6$) at a scan rate of 100 mV s^{-1} (working electrode: glassy carbon, counter electrode: Pt wire, reference electrode: saturated calomel electrode (SCE)). **BTBT(OMe)$_4$**, **BTBT(OMe)$_2$**, and BTBT show irreversible oxidation waves at 0.72, 0.88, and 1.18 V, respectively (Fig. S1). From the first onset oxidation potentials (E_{onset}), HOMO energies (E_{HOMO}) of **BTBT(OMe)$_4$**, **BTBT(OH)$_2$**, and BTBT were estimated to be −5.16, −5.32, and −5.62 V, respectively, by assuming the SCE energy level of −4.44 eV below the vacuum level.[18]

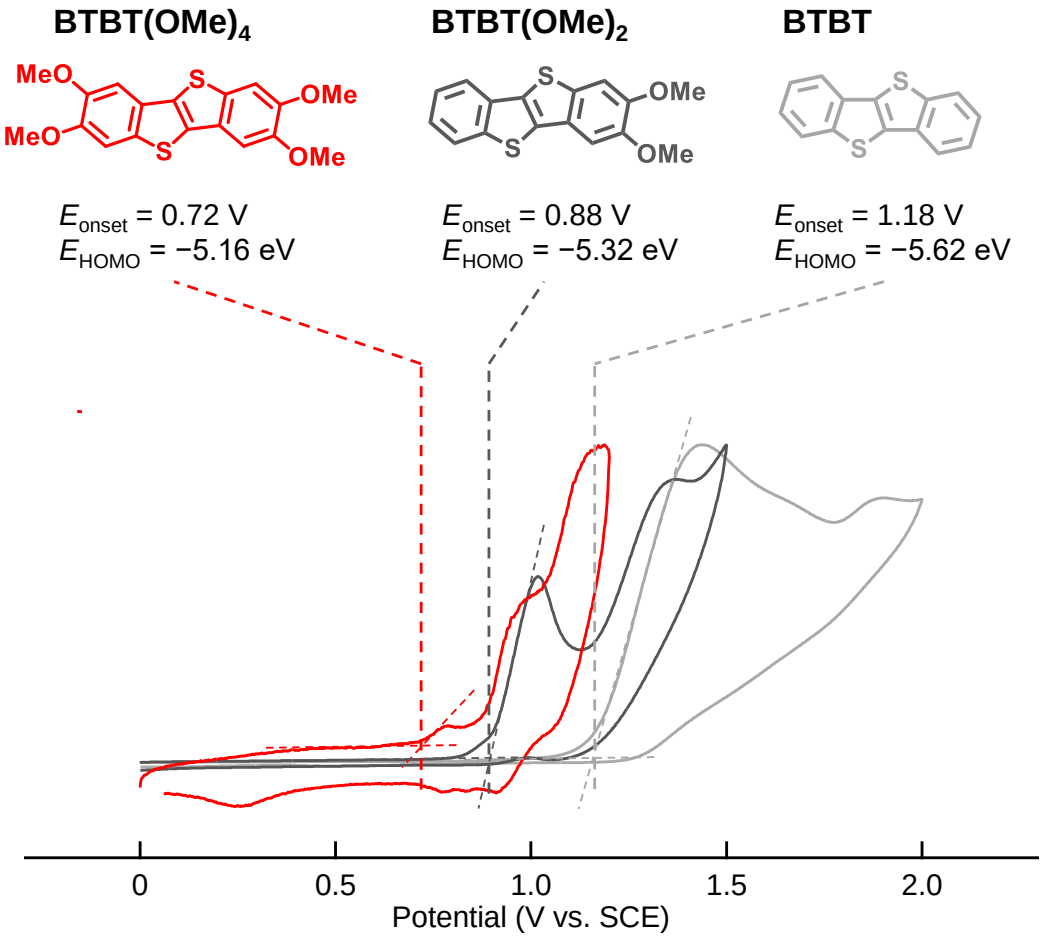

Fig. S1 Cyclic voltammograms of BTBT derivatives.

Optical properties

UV/vis spectra of **BTBT(OMe)$_2$** and **BTBT(OMe)$_4$** in a 10^{-5} M chloroform solution and a thin film deposited on a glass substrate were measured on a SHIMADZU UV-2450 UV-VIS spectrometer at room temperature (Fig. S2). In the solution, **BTBT(OMe)$_4$** (blue solid line) shows slightly longer wavelength absorptions (~355 nm) than **BTBT(OMe)$_2$** (red solid line, ~345 nm). This indicates that the π-conjugated system is certainly extended with increasing the number of attached methoxy groups, although the spectrum shapes of **BTBT(OMe)$_4$** and **BTBT(OMe)$_2$** are somewhat different from each other (especially in the longer wavelength region above 300 nm). Their spectra in the thin film state (dashed lines) are broadened and slightly red-shifted compared with those in solution, to give the longest wavelength absorption peak in a similar range (~350 nm). In addition, the spectral broadening in the **BTBT(OMe)$_2$** thin film is more significant than that in the **BTBT(OMe)$_4$** thin film. Considering the slipped dimer/tetramer structure in the crystal of **BTBT(OMe)$_2$** (Fig. 2), the formation of J-type aggregates in the **BTBT(OMe)$_2$** thin film is expected, which might cause the significant spectral broadening. Therefore, the differences in the aggregation properties of **BTBT(OMe)$_2$** and **BTBT(OMe)$_4$** attributable to the difference in the methoxy substitution manner (asymmetric or symmetric) would affect the optical properties in thin film.

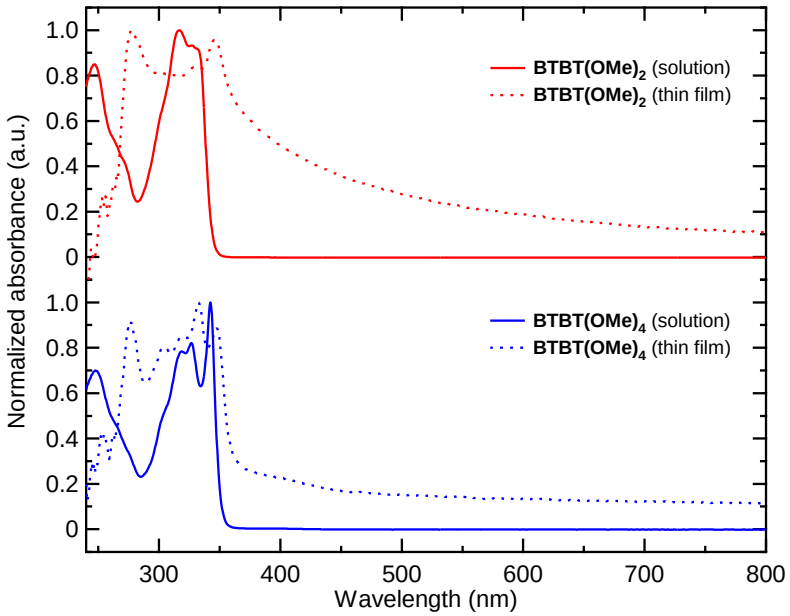

Fig. S2 UV/vis spectra of **BTBT(OMe)$_2$** (red) and **BTBT(OMe)$_4$** (blue) measured in a $CHCl_3$ solution (solid line) and a thin film (dashed line) at room temperature.

Crystal structures

· Data collection

The reflection data were collected on a Rigaku Mercury II CCD diffractometer with a graphite-monochromated MoKα radiation source (λ = 0.71073 Å). For indexing and integrating the diffraction peaks, the CrystalClear-SM program (Rigaku) was used. Empirical absorption correction was applied with the REQAB program.

· Analysis

The structures were solved by direct methods (SIR 2008) and refined by full-matrix least-squares by applying anisotropic temperature factors for all non-hydrogen atoms using the SHELX-97 programs.[S2] The hydrogen atoms were placed at geometrically calculated positions. Details on crystallographic X-ray data collections and refinements are found in Table S1.

Table S1 Crystallographic data.

Crystals	**BTBT(OMe)$_2$** [14]	**7**	**BTBT(OMe)$_4$**
Empirical formula	$C_{16}H_{12}O_2S_2$	$C_{18}H_{16}O_4S_3$	$C_{18}H_{16}O_4S_2$
Formula weight	300.39	392.50	360.44
Crystal shape	colourless plate	orange rod	colorless prism
Crystal size (mm^3)	0.20×0.17×0.036	0.15×0.12×0.085	0.14×0.14×0.020
Crystal system	triclinic	triclinic	monoclinic
Space group	*P*−1	*P*−1	$P2_1/c$
a (Å)	10.676(4)	8.573(3)	12.164(4)
b (Å)	10.861(4)	11.488(4)	8.759(3)
c (Å)	13.225(5)	18.172(7)	7.875(3)
α (°)	104.975(4)	95.972(5)	90
β (°)	102.681(4)	95.420(6)	97.646(4)
γ (°)	99.616(4)	90.091(6)	90
V (Å^3)	1404.0(9)	1771.9(11)	831.6(5)
Z	4	4	2
Unique refls. (R_{int})	4827 (0.0253)	6067 (0.0564)	1901 (0.0370)
D_{calc} (g/cm^3)	1.421	1.471	1.439
R_1	0.0566	0.0660	0.0495
R_w	0.1727	0.1977	0.1419
GOF	1.076	1.052	1.066
Temperature (K)	293	293	293
CCDC number	1529673	1539947	1539948

Rod-like orange crystals of compound **7** were obtained by a diffusion method of a dichloromethane/methanol solution. A crystal belongs to a triclinic system, space group *P*−1 (#2). Two molecules are crystallographically independent, and are twisted at the dithiin part with the dihedral angles of 26.9° and 27.4° between the phenyl group and the benzothienyl group (Fig. S3). A methoxy group in one molecule is disordered to two positions with occupancy 77% for the majority and 23% for minority. The unit cell contains four molecules. The molecules are dimerized along the (*b*+*c*−*a*) body diagonal direction and the resulting column structure is further stabilized by weak [C−H···O]-type H-bonds between the methoxy groups.

(a) Crystallographically independent molecules.

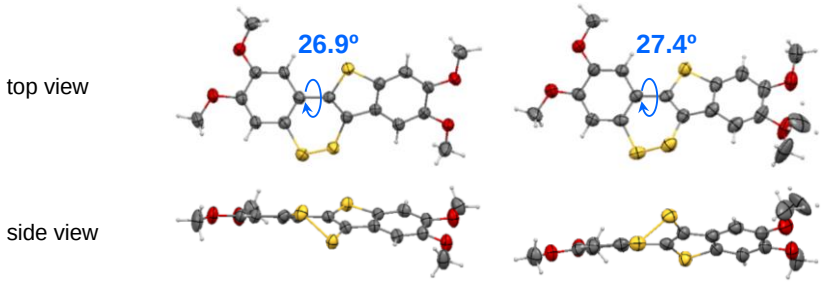

(b) Projection along the *a* axis.

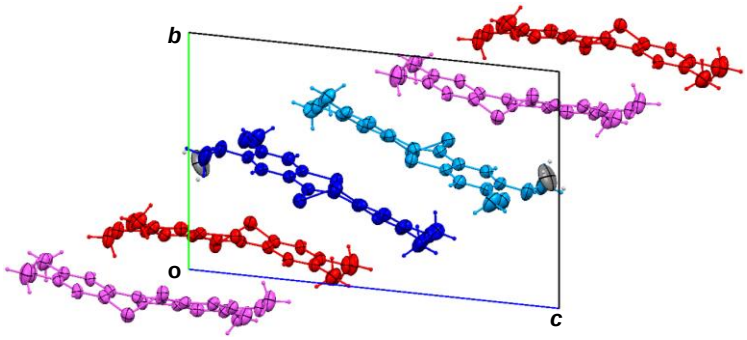

(b) Projection along the *b* axis.

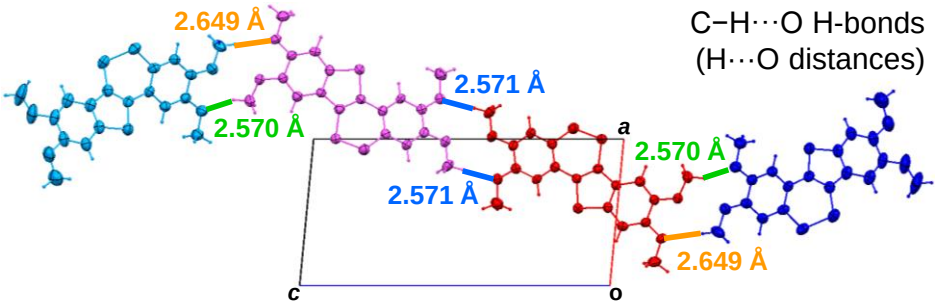

Fig. S3 Molecular structure and molecular arrangement of the dithiin compound **7**. The thermal ellipsoids are scaled to the 50% probability level.

Transfer integral calculations

Transfer integrals in the **BTBT(OMe)$_2$** and **BTBT(OMe)$_4$** crystals (Fig. 2) were estimated from the intermolecular overlap integrals of their HOMO calculated by the AM1 method.[20,26,S3]

Device fabrication

Thin-film and single-crystal transistors were fabricated onto n-doped Si substrates with a thermally grown SiO_2 dielectric layer (300 nm, C = 11.5 nF/cm^2). The SiO_2 surface (bare) was treated with hexamethyldisilazane (HMDS)[S4], octadecyltrimethoxysilane (OTMS)[S5], and polystyrene (PS, 100 nm)[S6]. The resulting overall capacitance of the gate dielectrics was 11.5 nF/cm^2 for HMDS and OTMS, and 7.6 nF/cm^2 for PS.[S7] For the thin-film device, the organic semiconductor, **BTBT(OMe)$_2$** or **BTBT(OMe)$_4$**, with a thickness of 50 nm was vacuum evaporated, and then the thin films were annealed at 100 °C for 12 h under vacuum. The top-contact source-drain electrodes were patterned by thermal deposition of gold using a shadow mask; the channel length (L) and width (W) were 50−200 μm and 1000 μm, respectively. The transistor characteristics were measured under ambient conditions, by using a semiconductor parameter analyzer. The mobility (μ), the threshold voltage (V_{th}), and the on/off ratio (I_{on}/I_{off}) were evaluated from the transconductance in the saturated region.

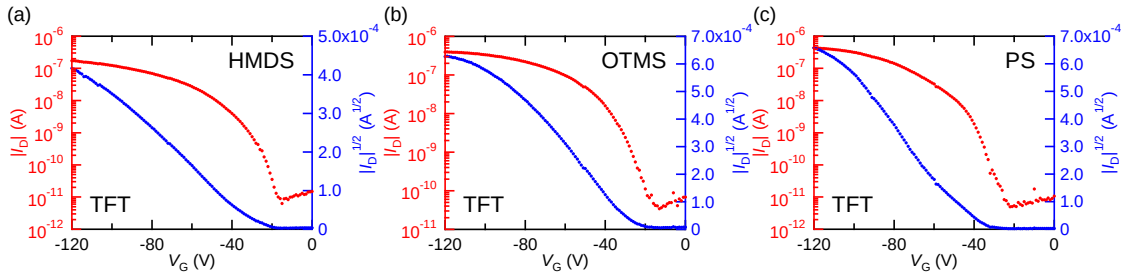

Fig. S4 Transfer characteristics of the **BTBT(OMe)$_4$**-based TFTs without thermal annealing, measured at V_D = −80 V: (a) HMDS, (b) OTMS, (c) PS.

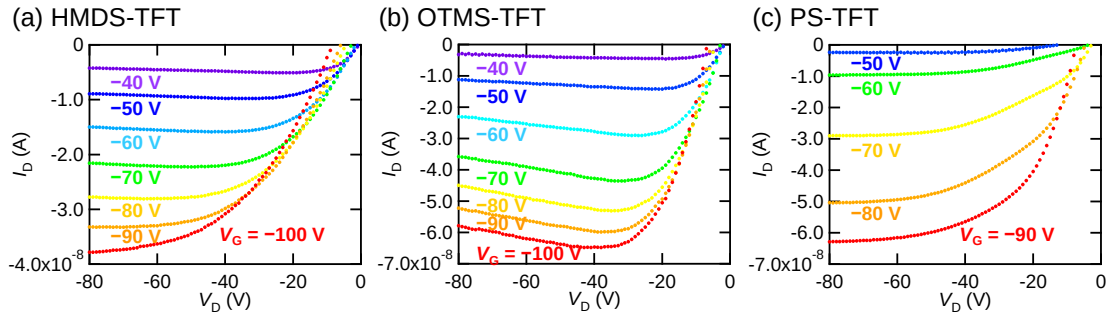

Fig. S5 Output characteristics of the **BTBT(OMe)$_4$**-based TFTs: (a) HMDS, (b) OTMS, (c) PS.

Thin-film properties

X-ray diffraction patterns of the **BTBT(OMe)$_2$** and **BTBT(OMe)$_4$** thin films (50 nm) deposited on the SiO_2 surface (bare) and the HMDS, OTMS, PS-treated substrates were obtained by a Rigaku SmartLab with a monochromated CuKα radiation (λ = 1.541838 Å) under ambient conditions.

Atomic force microscopy (AFM) images of the **BTBT(OMe)$_2$** and **BTBT(OMe)$_4$** thin films (50 nm) deposited on the SiO_2 surface (bare) and the HMDS, OTMS, PS-treated substrates were recorded on a Dimension 3000 Nanoscope IIIa (Bruker Co., Ltd., USA) in the tapping mode. The AFM images and the height profiles of the evaporated thin films with/without thermal annealing at 100 °C are shown in Fig. S6 and S7, respectively.

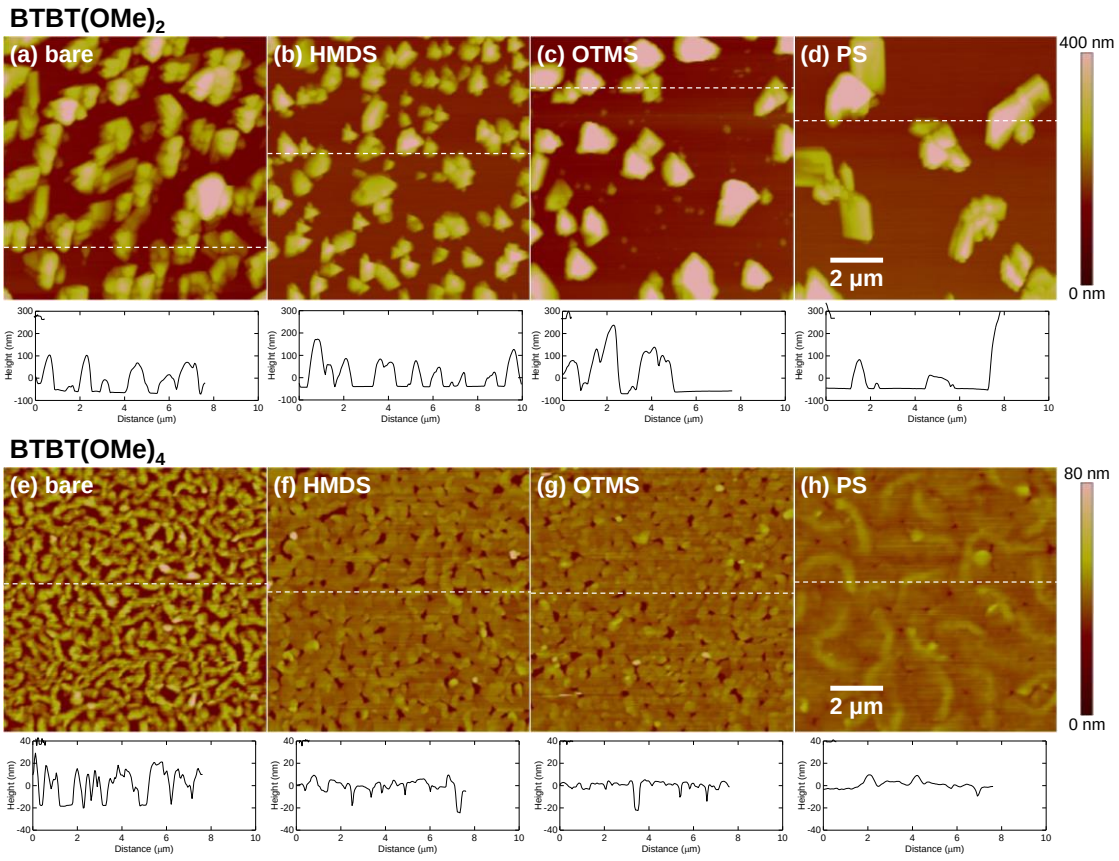

Fig. S6 AFM images (size: 10 μm × 10 μm) and the height profiles of the evaporated thin films based on **BTBT(OMe)$_2$** and **BTBT(OMe)$_4$**: (a, e) bare, (b, f) HMDS, (c, g) OTMS, and (d, h) PS. The height profiles are measured along the white dashed lines in the respective AFM images.

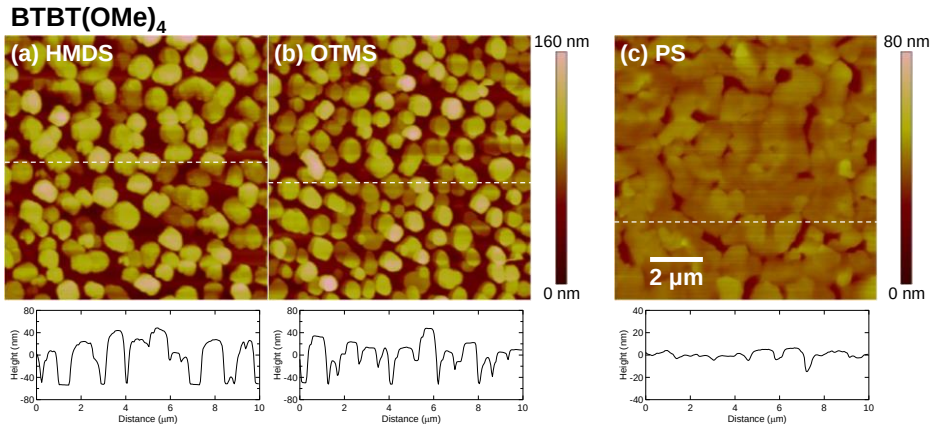

Fig. S7 AFM images (size: 10 μm × 10 μm) and the height profiles of the evaporated thin films based on **BTBT(OMe)$_4$**, after thermal annealing at 100 °C: (a) HMDS, (b) OTMS, and (c) PS. The height profiles are measured along the white dashed lines in the respective AFM images.

References

S1. M. J. Frisch, G. W. Trucks, H. B. Schlegel, G. E. Scuseria, M. A. Robb, J. R. Cheeseman, J. A. Montgomery, Jr., T. Vreven, K. N. Kudin, J. C. Burant, J. M. Millam, S. S. Iyengar, J. Tomasi, V. Barone, B. Mennucci, M. Cossi, G. Scalmani, N. Rega, G. A. Petersson, H. Nakatsuji, M. Hada, M. Ehara, K. Toyota, R. Fukuda, J. Hasegawa, M. Ishida, T. Nakajima, Y. Honda, O. Kitao, H. Nakai, M. Klene, X. Li, J. E. Knox, H. P. Hratchian, J. B. Cross, V. Bakken, C. Adamo, J. Jaramillo, R. Gomperts, R. E. Stratmann, O. Yazyev, A. J. Austin, R. Cammi, C. Pomelli, J. W. Ochterski, P. Y. Ayala, K. Morokuma, G. A. Voth, P. Salvador, J. J. Dannenberg, V. G. Zakrzewski, S. Dapprich, A. D. Daniels, M. C. Strain, O. Farkas, D. K. Malick, A. D. Rabuck, K. Raghavachari, J. B. Foresman, J. V. Ortiz, Q. Cui, A. G. Baboul, S. Clifford, J. Cioslowski, B. B. Stefanov, G. Liu, A. Liashenko, P. Piskorz, I. Komaromi, R. L. Martin, D. J. Fox, T. Keith, M. A. Al-Laham, C. Y. Peng, A. Nanayakkara, M. Challacombe, P. M. W. Gill, B. Johnson, W. Chen, M. W. Wong, C. Gonzalez and J. A. Pople, GAUSSIAN 03 (Revision E.01), Gaussian, Inc., Wallingford CT, 2004.

S2. (a) M. C. Burla, R. Caliandro, M. Camalli, B. Carrozzini, G. L. Cascarano, L. de Caro, C. Giacovazzo, G. Polidori, D. Siliqi, R. Spagna, *J. Appl. Crystallogr.*, 2007, **40**, 609; (b) G. M. Sheldrick, *Acta Crystallogr., Sect. A: Found. Crystallogr.*, 2008, **A64**, 112.

S3. http://www.op.titech.ac.jp/lab/mori/lib/program.html

S4. T. Yamao, K. Juri, A. Kamoi and S. Hotta, *Org. Electron.*, 2009, **10**, 1241.

S5. Y. Ito, A. A. Virkar, S. Mannsfeld, J. H. Oh, M. Toney, J. Locklin and Z. Bao, *J. Am. Chem. Soc.*, 2009, **131**, 9396.

S6. M.-H. Yoon, H. Yan, A. Facchetti and T. J. Marks, *J. Am. Chem. Soc*., 2005, **127**, 10388.

S7. K.-J. Baeg, Y.-Y. Noh, J. Ghim, B. Lim and D.-Y. Kim, *Adv. Funct. Mater.*, 2008, **18**, 3678.